

See discussions, stats, and author profiles for this publication at: <https://www.researchgate.net/publication/231273851>

Critical Nanoaggregate Concentration of Asphaltenes by Direct-Current (DC) Electrical Conductivity†

ARTICLE *in* ENERGY & FUELS · MARCH 2009

Impact Factor: 2.79 · DOI: 10.1021/ef800781a

CITATIONS

53

READS

39

4 AUTHORS, INCLUDING:



Huang Zeng

BP plc

29 PUBLICATIONS 760 CITATIONS

SEE PROFILE



Oliver C Mullins

Schlumberger Limited

245 PUBLICATIONS 6,003 CITATIONS

SEE PROFILE

Article

Critical Nanoaggregate Concentration of Asphaltenes by Direct-Current (DC) Electrical Conductivity

Huang Zeng, Yi-Qiao Song, David L. Johnson, and Oliver C. Mullins

Energy Fuels, **2009**, 23 (3), 1201-1208 • DOI: 10.1021/ef800781a • Publication Date (Web): 29 January 2009

Downloaded from <http://pubs.acs.org> on May 11, 2009

More About This Article

Additional resources and features associated with this article are available within the HTML version:

- Supporting Information
- Access to high resolution figures
- Links to articles and content related to this article
- Copyright permission to reproduce figures and/or text from this article

[View the Full Text HTML](#)



ACS Publications
High quality. High impact.

Energy & Fuels is published by the American Chemical Society, 1155 Sixteenth Street N.W., Washington, DC 20036

Critical Nanoaggregate Concentration of Asphaltenes by Direct-Current (DC) Electrical Conductivity[†]

Huang Zeng,* Yi-Qiao Song, David L. Johnson, and Oliver C. Mullins

Schlumberger-Doll Research, Cambridge, Massachusetts 02139

Received September 17, 2008. Revised Manuscript Received January 2, 2009

The critical nanoaggregate concentration (CNAC) of asphaltenes in toluene has been studied by a variety of methods recently. Here, we explore low-frequency electrical impedance measurements to detect and quantify nanoaggregate formation of asphaltenes. The Nyquist and Bode plots confirm the frequency range necessary for the dominance of (organic) ion conduction as opposed to reactive impedance. Impedance measurements are made as a function of the asphaltene concentration in toluene. We perform ionic conduction measurements at low frequency to avoid electrode polarization effects and then extrapolate to obtain direct-current (DC) conductivity. In a plot of DC conductivity versus asphaltene concentration, we see a clear break between two linear regions that is attributed to nanoaggregate formation. Very close agreement with high-Q ultrasonic measurements is shown for two petroleum asphaltenes with different CNACs. In addition, this work is shown to be consistent with previous alternating-current (AC) conductivity measurements. Measurements on aqueous salt solutions are used to validate measurements of the mole fraction of asphaltenes ionized in toluene, which is $\sim 10^{-5}$. The plausible identity of these ions is discussed. A comparison of conductivity at concentrations below and above CNAC indicates that the aggregation number is small (<10) in agreement with previous findings. Resin shows no aggregation and is also much less conductive than asphaltenes. We also observe a break in the slope at higher asphaltene concentrations, where nanoaggregate clustering has been observed.

Introduction

Asphaltenes are the most aromatic and complex component of crude oils; large mass fractions of asphaltenes are the defining characteristic of heavy oils and bitumens.¹ Asphaltenes also appear to play an important role in the global carbon cycle; derivitized, ionic asphaltenes are evidently found in oceans at the gigaton quantity.² Indeed, compounds of similar chemical structure are found in aqueous extracts of crude oil.³ By any measure, asphaltenes are very important in a variety of ways. As such, it is essential to work out the chemical and physical properties of asphaltenes. In particular, understanding the aggregation characteristics of asphaltenes is central for efficient resource use and is the focus herein. It is now within reach to understand these properties from a first-principles vantage. We briefly address asphaltene molecular structure and relate this to nanoaggregation.

Previous reports of asphaltene molecular weights differed by orders of magnitude; fortunately, this situation is resolved. Two primary methods have been decisive to resolve the controversy: molecular diffusion and mass spectroscopy. Time-resolved fluorescence depolarization (TRFD) studies by Groenzin and co-workers have indicated that most likely petroleum asphaltene

molecular weights are ~ 750 Da with a full width at half-maximum of 500–1000 Da.^{4–7} Taylor dispersion measurements by Wargadalam and co-workers of coal-derived asphaltenes are in close agreement with TRFD studies.⁸ Nuclear magnetic resonance (NMR) diffusion measurements by Freed and co-workers give comparable molecular sizes.⁹ The NMR distributions had a somewhat large high mass tail, possibly explained by the fact that the lowest concentration of asphaltenes that has been investigated is already in the range of dimer formation.^{7,10} Fluorescence correlation spectroscopy (FCS) by Andrews and co-workers has yielded results comparable to TRFD and, in particular, shows that coal asphaltenes are $1/2$ in size in comparison to petroleum asphaltenes,^{11–13} in agreement with other studies.

(4) Groenzin, H.; Mullins, O. C. Asphaltene molecular size and structure. *J. Phys. Chem. A* **1999**, *103*, 11237–11245.

(5) Groenzin, H.; Mullins, O. C. Molecular sizes of asphaltenes from different origin. *Energy Fuels* **2000**, *14*, 677–684.

(6) Buenrostro-Gonzalez, E.; Groenzin, H.; Lira-Galeana, C.; Mullins, O. C. The overriding chemical principles that define asphaltenes. *Energy Fuels* **2001**, *15*, 972–978.

(7) Badre, S.; Goncalves, C. C.; Norinaga, K.; Gustavson, G.; Mullins, O. C. Molecular size and weight of asphaltene and asphaltene solubility fractions from coals, crude oils and bitumen. *Fuel* **2006**, *85*, 1–11.

(8) Wargadalam, V. J.; Norinaga, K.; Iino, M. Size and shape of a coal asphaltene studied by viscosity and diffusion coefficient measurements. *Fuel* **2002**, *81*, 1403–1407.

(9) Freed, D. E.; Lisitz, N. V.; Sen, P. N.; Song, Y. Q. Asphaltene molecular composition and dynamics from NMR diffusion measurements. In *Asphaltene, Heavy Oils and Petroleomics*; Mullins, O. C., Sheu, E. Y., Hammami, A., Marshall, A. G., Eds.; Springer: New York, 2007; Chapter 11.

(10) Goncalves, S.; Castillo, J.; Fernandez, A.; Hung, J. Absorbance and fluorescence spectroscopy on the aggregation behavior of asphaltene toluene solutions. *Fuel* **2004**, *83*, 1823–1828.

(11) Guerra, R.; Ladavac, K.; Andrews, A. B.; Sen, P. N.; Mullins, O. C. Diffusivity of coal and petroleum asphaltenes monomers by fluorescence correlation spectroscopy. *Fuel* **2007**, *86*, 2016–2020.

[†] Presented at the 9th International Conference on Petroleum Phase Behavior and Fouling.

* To whom correspondence should be addressed. E-mail: hzeng@exchange.slb.com.

(1) *Asphaltene, Heavy Oils and Petroleomics*; Mullins, O. C., Sheu, E. Y., Hammami, A., Marshall, A. G., Eds.; Springer: New York, 2007.

(2) Koch, T.; Dittmar, T. Thermogenic organic matter dissolved in the abyssal ocean. *Mar. Chem.* **2006**, *102*, 208–217.

(3) Stanford, L. A.; Kim, S.; Klein, G. C.; Smith, D. F.; Rodgers, R. P.; Marshall, A. G. Identification of water-soluble heavy crude oil organic acids, bases, and neutrals by electrospray ionization and field desorption ionization Fourier transform ion cyclotron resonance mass spectrometry. *Environ. Sci. Technol.* **2007**, *41*, 2696–2702.

Mass spectroscopy has played a crucial role in resolving asphaltene molecular weight. Boduszynski employed field ionization mass spectroscopy to obtain most likely asphaltene molecular weights of ~ 800 Da.¹⁴ Qian and co-workers obtained similar but somewhat higher results by field desorption mass spectroscopy.¹⁵ Marshall and co-workers have published extensively on asphaltenes and related materials.^{3,16,17} They obtain asphaltene molecular weights in very close agreement with the TRFD work. Laser desorption ionization has been problematic,¹⁸ in that conflicting reports have appeared. Martínez-Haya and co-workers have resolved this issue, showing that gas-phase aggregation of asphaltenes can introduce massive artifacts without proper experimental control.^{19,20} More recently, Pomerantz and co-workers have confirmed this finding by employing two separate lasers in LDI experiments, called two-step laser desorption ionization (L2MS): an IR laser for desorption and a UV laser for ionization of molecules in the neutral plume.^{21,22} The L2MS studies show independence of the asphaltene molecular-weight profile on the power of either laser, the timing of ion collection, and the surface concentration of asphaltenes.^{21,22} All mass spectral techniques show that most likely asphaltene molecular weights are ~ 750 Da, with different techniques within a 20% range of this number.

A second, currently unresolved question is that of asphaltene molecular architecture; in particular, the question arises how many polycyclic aromatic hydrocarbon (PAH) ring systems are there per asphaltene molecule? The first reports and for many years the only reports that asphaltenes possess predominantly a single PAH ring system per molecule were issued in the TRFD studies.^{4–7} The rotational diffusion rates of small, blue-emitting asphaltene fluorophores are 10 times those of large, red-emitting asphaltene fluorophores; evidently they are not cross-linked. Moreover, the fluorescence quantum yield of all crude oils

including the very asphaltene rich have been shown to obey the energy gap law;²³ thus, there is no indication that particular classes of asphaltene molecules are being excluded in these studies. The TRFD studies were central to change the previously prevailing view of large, polymeric asphaltene molecules; their second important find regarding the number of PAHs per molecule should be carefully considered. Indeed, a PAH consisting of seven rings with 55% alkane (known for petroleum asphaltenes) and a sulfur atom is roughly the most likely molecular weight of asphaltene; therefore, one PAH per molecule seems like a natural conclusion. Analysis of the optical absorption and emission properties of asphaltenes coupled with extensive molecular-orbital (MO) calculations on more than 500 different PAH molecules provides strong corroboration of a single PAH per molecule.^{24–26} Recently, gas-phase single-molecule decomposition studies have provided very strong evidence for the dominance of asphaltene molecules with a single PAH.²⁷ These important studies show that molecular fragmentation induced by collision with helium does indeed result in the loss of carbon but with predominantly no change in aromaticity. This result has been established for several molecular classes of asphaltenes, such as single basic nitrogen- and single acidic nitrogen-containing molecules. This result is found in all molecular-weight ranges of asphaltenes including the high mass tail, implying the existence of a small mass fraction of asphaltenes with a single, large fused ring system. This is in accordance with the optical/MO studies that concluded that PAHs with up to 15 rings are plausibly present in asphaltenes but in small mass fraction.^{25,26} It is probably not coincidental that the evident asphaltene-derived compounds found in the oceans have been shown to possess seven fused aromatic ring systems on average.² Asphaltene molecular architecture is likely related to asphaltene nanoaggregate formation, as will be discussed shortly.

A third area of previously unresolved questions in asphaltene science relates to aggregation; in particular, it concerns the concentration of asphaltene in toluene at which aggregation starts as well as the nature of these aggregates. There had been several reports claiming that the “critical micelle concentration” (CMC) of asphaltenes in toluene is around several grams per liter. For most of these studies, surface tension versus concentration was used, a method well-known for CMC determination in aqueous systems. However, it was pointed out that these results are necessarily misinterpreted;²⁸ loading high-energy molecules on the surface of a low surface tension solvent, such as toluene, would increase and not decrease the surface tension as reported.

In early work, the aggregation concentration of asphaltenes in pyridine has been reported to be roughly $1/2$ g/L.²⁹ Indeed, the higher surface tension of pyridine (38 dynes/cm) than that

(12) Schneider, M. H.; Andrews, A. B.; Mitra-Kirtley, S.; Mullins, O. C. Asphaltene molecular size by fluorescence correlation spectroscopy. *Energy Fuels* **2007**, *21*, 2875–2882.

(13) Andrews, A. B.; Shih, W. C.; Edwards, J.; Norinaga, K.; Mullins, O. C. Coal asphaltene molecular size by fluorescence correlation spectroscopy. *Energy Fuels* **2009**, manuscript submitted.

(14) Boduszynski, M. M. In *Chemistry of Asphaltenes*; Bunger, J. W., Li, N. C., Eds.; American Chemical Society: Washington, D.C., 1981; Chapter 7.

(15) Qian, K.; Edwards, K. E.; Siskin, M.; Olmstead, W. N.; Mennito, A. S.; Dechert, G. J.; Hoosain, N. E. Desorption and ionization of heavy petroleum molecules and measurement of molecular weight distributions. *Energy Fuels* **2007**, *21* (2), 1042–1047.

(16) Rodgers, R. P.; Marshall, A. G. Petroleumomics: Advanced characterization of petroleum derived materials by Fourier transform ion cyclotron resonance mass spectrometry (FT-ICR MS). In *Asphaltene, Heavy Oils and Petroleumomics*; Mullins, O. C., Sheu, E. Y., Hammami, A., Marshall, A. G., Eds.; Springer: New York, 2007; Chapter 3.

(17) Klein, G. C.; Kim, S.; Rodgers, R. P.; Marshall, A. G.; Yen, A.; Asomaning, S. Mass spectral analysis of asphaltenes. I. Compositional differences between pressure-drop and solvent-drop asphaltenes determined by electrospray ionization Fourier transform ion cyclotron resonance mass spectrometry. *Energy Fuels* **2006**, *20*, 1965–1972.

(18) Mullins, O. C.; Martínez-Haya, B.; Marshall, A. G. Contrasting perspective on asphaltene molecular weight. This Comment vs the overview of A. A. Herod, K. D. Bartle, and R. Kandiyoti. *Energy Fuels* **2008**, *22*, 1765–1773.

(19) Martínez-Haya, B.; Hortal, A. R.; Hurtado, P. M.; Lobato, M. D.; Pedrosa, J. M. Laser desorption/ionization determination of molecular weight distributions of polyaromatic carbonaceous compounds and their aggregates. *J. Mass Spectrom.* **2007**, *42*, 701–713.

(20) Hortal, A. R.; Hurtado, P. M.; Martínez-Haya, B.; Mullins, O. C. Molecular weight distributions of coal and petroleum asphaltenes from laser desorption ionization experiments. *Energy Fuels* **2007**, *21*, 2863–2868.

(21) Pomerantz, A. E.; Hammond, M. R.; Morrow, A. L.; Mullins, O. C.; Zare, R. N. Two-step laser mass spectrometry of asphaltenes. *J. Am. Chem. Soc.* **2008**, *130*, 7216–7217.

(22) Pomerantz, A. E.; Hammond, M. R.; Morrow, A. L.; Mullins, O. C.; Zare, R. N. Asphaltene molecular-mass distribution determined by two-step laser mass spectrometry. *Energy Fuels* **2009**, in press.

(23) Ralston, C. Y.; Wu, X.; Mullins, O. C. Quantum yields of crude oils. *Appl. Spectrosc.* **1996**, *50*, 1563–1568.

(24) Ruiz-Morales, Y.; Mullins, O. C. Polycyclic aromatic hydrocarbons of asphaltenes analyzed by molecular orbital calculations with optical spectroscopy. *Energy Fuels* **2007**, *21*, 256–265.

(25) Ruiz-Morales, Y.; Wu, X.; Mullins, O. C. Electronic absorption edge of crude oils and asphaltenes analyzed by molecular orbital calculations with optical spectroscopy. *Energy Fuels* **2007**, *21*, 944–952.

(26) Ruiz-Morales, Y.; Mullins, O. C. Measured and simulated electronic absorption and emission spectra of asphaltenes. *Energy Fuels* **2009**, in press.

(27) McKenna, A. M.; Purcell, J. M.; Rodgers, R. P.; Marshall, A. G. Atmospheric pressure photoionization Fourier transform ion cyclotron resonance mass spectrometry for detailed compositional analysis of petroleum. Presented at the 9th International Conference on Petroleum Phase Behavior and Fouling, Victoria, British Columbia, Canada, June 15–19, 2008; Abstract 17.

(28) Friberg, S. E.; Mullins, O. C.; Sheu, E. Y. Surface activity of an amphiphilic association structure. *J. Dispersion Sci. Technol.* **2005**, *26*, 513–515.

of toluene (28 dynes/cm) might be sufficient to overcome limitations noted for determination of CNAC by surface tension in organic solvents.²⁸ Optical fluorescence methods have reported the onset of aggregation in toluene,¹⁰ and this work has been confirmed subsequently.³⁰

However, optical fluorescence methods are likely not able to differentiate between the dimer and aggregate formations of asphaltenes.³⁰ In particular, with an increasing concentration, asphaltenes go from true molecular solutions, dimers, nanoaggregates, to eventually clusters of nanoaggregates. There is a range of concentration where dimers first start to form and where nanoaggregates start to form.³⁰ We use the terminology that, with increasing concentration, dimer formation corresponds to the onset of aggregation, while the critical nanoaggregate concentration corresponds to the termination of nanoaggregate growth.

The first reports that the critical nanoaggregate concentration of asphaltenes in toluene (CNAC) is actually much lower than previous reports were obtained from high- Q ultrasonic studies by Andreatta and co-workers^{30,31} [The terminology was changed by the asphaltene community from “micelle” to “nanoaggregate” reflecting the lack of any emulsifying agent, among other differences. Professor Johan Sjöblom, Norwegian University of Science and Technology (NTNU), suggested this change. This terminology change has implicit rejection of the concept of peptizing resins]. The CNAC of asphaltenes in toluene was found to be ~ 100 mg/L. In addition, these studies indicated that, unlike other non-ionic surfactants in organic solvents, the asphaltene nanoaggregate size remains fixed.^{30,31} This property of fixed micelle size is observed for aqueous surfactants. These results for asphaltenes were quickly confirmed by NMR hydrogen index measurements, which showed a clear break at ~ 200 mg/L.⁹ In addition, NMR translational diffusion measurements indicated a change in diffusion constant at this concentration with a factor of 2 reduction in magnitude.⁹ Because the translational diffusion constant is inversely proportional to the radius, this would correspond roughly to eight molecules in nanoaggregate. Alternating-current (AC) conductivity measurements performed by Eric Sheu and co-workers showed a break in the conductivity curve at ~ 150 mg/L, confirming the high- Q ultrasonics and NMR measurements.³² These AC conductivity measurements have been confirmed in another laboratory.³³ Gravitational gradients in oil reservoirs have confirmed the presence of asphaltene nanoaggregates in crude oils,^{34,35} and aggregation numbers of ~ 8 were found.³⁵ Centrifugation studies have clearly shown enormous changes in asphaltene aggregation in the ~ 50 mg/L range for a particular petroleum asphaltene, providing robust corroboration of the many nanoaggregate studies.³⁶ All of these studies are consistent with the general find in small-angle neutron scattering (SANS) and small-angle

X-ray scattering (SAXS) studies of a rather small invariant particle in asphaltenes.^{37–40} Of course, the SAXS and SANS studies find structures of various length scales in asphaltene systems. Nevertheless, a compelling result from SAXS is the presence of nanoaggregates in asphaltenes but not in resins.³⁷

Several of these studies, including the high- Q ultrasonics and the NMR studies, indicate little or no change in the size of the asphaltene nanoaggregates at least up to ~ 1 g/L concentration, an observation consistent with the SAXS and SANS studies.^{37–40} An explanation has been advanced founded in asphaltene molecular architecture.⁶ The attractive component in asphaltene molecules is van der Waals forces primarily associated with the single, large PAH of the molecule. Asphaltene nitrogen has been shown to be entirely aromatic and is the site of some charge separation enhancing interaction energy.⁴¹ The primary repulsive part of asphaltene molecules is steric repulsion associated with the peripheral alkane chains.⁶ The disruption in stacking because of alkane chains has been shown by high-resolution transmission electron microscopy (HRTEM) in model compounds.⁴² The HRTEM studies also show that asphaltene molecular images exhibit the same type of stacking disruption.⁴² The asphaltenes, a solubility class, must have a balance of intermolecular attractive and repulsive forces. Coal-derived asphaltenes are roughly $1/2$ in size compared to petroleum asphaltenes. This has been shown by molecular diffusion measurements TRFD^{5–7} and FCS^{11,13} and mass spectrometer measurements LDI²⁰ and L2MS.²² Coal-sourced asphaltenes lack alkane, especially when obtained from resid from distillation of coal liquefaction products. Correspondingly, the repulsive component of coal asphaltenes is reduced. Consequently, the attractive component must likewise be reduced by reducing the size of the PAH ring system. This observation is confirmed directly by molecular-weight measurements^{5–7,11,13,20,22} as well as fluorescence spectral measurements⁶ and ^{13}C NMR analysis.⁶ In addition, HRTEM showed that the PAHs of coal-derived asphaltenes are much smaller than the petroleum asphaltene PAHs.⁴² The importance for asphaltene nanoaggregate formation is that, after aggregation of a few molecules (~ 8), access to the PAHs in a nanoaggregate is precluded; thus, additional asphaltene molecules form new nanoaggregates. At higher concentrations of several grams per

(29) Sheu, E. Y. Colloidal properties of asphaltenes in organic solvents. In *Asphaltene—Fundamentals and Applications*; Sheu, E. Y., Mullins, O. C., Eds.; Plenum: New York, 1995; also see references therein.

(30) Andreatta, G.; Goncalves, C. C.; Buffin, G.; Bostrom, N.; Quintella, C. M.; Arteaga-Larios, F.; Perez, E.; Mullins, O. C. Nanoaggregates and structure—function relations in asphaltenes. *Energy Fuels* **2005**, *19*, 1282–1289.

(31) Andreatta, G.; Bostrom, N.; Mullins, O. C. High- Q ultrasonic determination of the critical nanoaggregate concentration of asphaltenes and the critical micelle concentration of standard surfactants. *Langmuir* **2005**, *21*, 2728–2736.

(32) Sheu, E. Y.; Long, Y.; Hamza, H. Asphaltene self-association and precipitation in solvents—AC conductivity measurements. In *Asphaltene, Heavy Oils and Petroleomics*; Mullins, O. C., Sheu, E. Y., Hammami, A., Marshall, A. G., Eds.; Springer: New York, 2007; Chapter 10.

(33) Goual, L. Impedance Spectroscopy of Petroleum Fluids at Low Frequency. *Energy Fuels*, in press.

(34) Mullins, O. C.; Betancourt, S. S.; Cribbs, M. E.; Creek, J. L.; Andrews, B. A.; Dubost, F.; Venkataramanan, L. The colloidal structure of crude oil and the structure of reservoirs. *Energy Fuels* **2007**, *21*, 2785–2794.

(35) Betancourt, S. S.; Ventura, G. T.; Pomerantz, A. E.; Vilorio, O.; Dubost, F. X.; Zuo, J.; Monson, G.; Bustamante, D.; Purcell, J. M.; Nelson, R. K.; Rodgers, R. P.; Reddy, C. M.; Marshall, A. G.; Mullins, O. C. Nanoaggregates of asphaltenes in a reservoir crude oil and reservoir connectivity. *Energy Fuels* **2009**, in press.

(36) Mostowfi, F.; Indo, K.; Mullins, O. C.; McFarlane, R. Asphaltene nanoaggregates studied by centrifugation. *Energy Fuels* **2009**, in press.

(37) Sheu, E. Y. Petroleomics and characterization of asphaltene aggregates using small angle scattering. In *Asphaltene, Heavy Oils and Petroleomics*; Mullins, O. C., Sheu, E. Y., Hammami, A., Marshall, A. G., Eds.; Springer: New York, 2007; Chapter 14.

(38) Barre, L.; Simon, S.; Palermo, T. Solution properties of asphaltenes. *Langmuir* **2008**, *24* (8), 3709–3717.

(39) Fenistein, D.; Barre, L.; Espinat, D.; Livet, A.; Roux, J.-N.; Scarcella, M. Viscosimetric and neutron scattering study of asphaltene aggregates in mixed toluene/heptane solvents. *Langmuir* **1998**, *14*, 1013–1020.

(40) Gawrys, K.; Kilpatrick, P. Asphaltene aggregates are polydisperse oblate cylinders. *J. Colloid Interface Sci.* **2005**, *288*, 325–334.

(41) Mitra-Kirtley, S.; Mullins, O. C.; Chen, J.; van Elp, J.; George, S. J.; Cramer, S. P. Determination of the nitrogen chemical structures in petroleum asphaltenes using XANES spectroscopy. *J. Am. Chem. Soc.* **1993**, *115*, 252–258.

(42) Sharma, A.; Groenzin, H.; Tomita, A.; Mullins, O. C. Probing order in asphaltenes and aromatic ring systems by HRTEM. *Energy Fuel* **2002**, *16*, 490–496.

liter, nanoaggregates are thought to form clusters.^{43,44} This conclusion derives from the change of flocculation kinetics from diffusion-limited aggregation to reaction-limited aggregation (RLA) upon cluster formation.⁴³ RLA kinetics can occur if surface morphological rearrangement is necessary for adherence as is plausible for nanoaggregate clusters. Indeed, the decrease in surface tension with increasing concentration above CNAC is consistent with recent findings that inverse micelles loading onto the surface of organic solvents reduce surface tension.⁴⁵

Asphaltenes can now be understood within the “modified Yen model”.⁴⁶ The modifications to the original Yen model include an understanding of asphaltene molecular architecture and the direct connection of the architecture with the nanoaggregate formation. Moreover, the fact that the asphaltene molecules have the attractive part in the molecular interior and the repulsive part on the exterior indicates that nanoaggregate growth should shut off with a small aggregation number. It is very important to test these predictions regarding asphaltene nanoaggregates to test the foundations of petroleomics.

There is now a general framework to understand asphaltene structure–function relations. This is the founding principle of the new field petroleomics.¹ All components of this framework must be tested to establish validity and to enhance predictive capabilities. In particular, the CNAC of asphaltenes must be tested. In this report, we measure the conductivity of asphaltenes in toluene over a concentration range, including the previously reported CNAC. Two petroleum asphaltenes are used that have been studied by various other methods. The frequency dependence of the impedance is determined over a very large frequency range to assess where the conductivity of the asphaltene solution is dominated by the resistive term without a significant capacitive component. The Nyquist and Bode plots are obtained to assess the desired low-frequency limit and additionally to provide stringent tests for the validity of the measurements and interpretation. That is, the Nyquist and Bode plots are used to verify that our measurements are only sensitive to the resistive and not a reactive component of the impedance. In the present work, we propose a simple model to account for the low-frequency conductivity data and to provide a rough estimate of the aggregation number. The standard micelle theory that presumes monodispersity does not apply herein. The model depends upon the ionic component of dissolved asphaltenes in toluene being a very small mass fraction, which is confirmed by simple analysis. Aqueous solutions with small quantities of sodium chloride confirm this analysis. Conductivity of resins and asphaltenes are compared.

AC conductivity measurements have been employed for asphaltene studies previously by Fotland et al.⁴⁷ and Sheu and colleagues.³² To obtain the resistivity values of asphaltene solutions, Fotland et al. used the impedance values measured

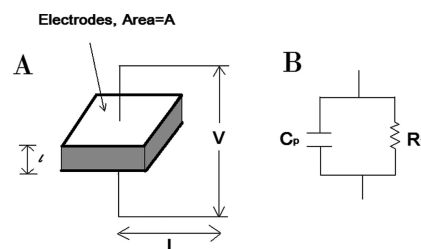


Figure 1. (A) Experimental apparatus for electric conductivity measurements. The surface area of the plate electrodes is A , and the distance between electrodes is l . (B) Parallel R – C circuit is suitable to be used as the equivalent circuit for this parallel plate method.

at a single frequency (1 KHz) and Sheu used the real part of impedance values measured at frequency ranging from 562 Hz to 13 MHz. As discussed in the Experimental Section below, at these relatively high frequencies, the measured impedance values will have significant contributions from the capacitive component. Therefore, the measured impedance or real part of the impedance will differ from the intrinsic resistivity. In our studies, the impedance analysis was conducted over a broader frequency range between 40 Hz and 15 MHz and the effects of the resistive and capacitive components were taken into account to give DC resistivity values. This allowed us to extract reliable values of resistivity and dielectric constant values.

Experimental Section

Materials. Two petroleum asphaltenes were measured in this study. The first sample was extracted from Burgan-5 (BG5) crude oil from Kuwait. The second sample was extracted from UMM-Gudair 8 (UG8) crude oil, which was also from Kuwait.

The procedure of asphaltene extraction is as follows: 100 mL of crude oil was diluted in 4 L *n*-heptane (99%, from Sigma-Aldrich, St. Louis, MO) and stirred at room temperature (21 °C) in darkness for 24 h. Then, the precipitated asphaltene was vacuum-filtered using a nylon membrane filter with pores of 0.45 μ m (Pall Life Science, East Hills, NY) and washed with enough *n*-heptane until the solvent was colorless. Then, the asphaltene was dissolved into 100 mL of toluene (99%, Sigma-Aldrich, St. Louis, MO), diluted in 4 L *n*-heptane, and again stirred for 24 h. After that, the precipitated asphaltene was filtered again and washed until the solvent was colorless. In the end, the asphaltene was dried in air and stored in an aluminum-foil-covered container.

The deasphaltene crude oil–heptane solution was evaporated to remove most of the heptane first and then loaded onto the top of a flash chromatography column filled with silica gel (Silica Gel 60, Sigma-Aldrich, St. Louis, MO) and flushed with a toluene/methanol (90:10 vol) mixture. The first colored portion flushed out of the column was collected, and the solvents were evaporated to obtain the resin component of the oil.

When preparing solutions, the appropriate amount of asphaltene was weighed and dissolved into toluene (99.8%, anhydrous, from Sigma) solution at a concentration of 10 g/L. Then, this stock solution was used to make asphaltene solutions at lower concentrations. In this study, asphaltene–toluene solutions of 10, 5, 2, 1, 0.5, 0.4, 0.3, 0.2, 0.15, 0.1, 0.075, 0.05, 0.035, 0.02, and 0.01 g/L were prepared and kept still at 21 °C in darkness. After about 24 h, the samples were used for measurement.

The sodium chloride used in this study was of ACS reagent grade from Sigma-Aldrich. The water was also of ACS reagent grade from Sigma-Aldrich.

Methods. Impedance measurements on high impedance materials are often performed using two-terminal connections.⁴⁸ The impedance measurements were conducted using a commercial two-

(43) Yudin, I. K.; Anisimov, M. A. Dynamic light scattering monitoring of asphaltene aggregation in crude oils and hydrocarbon solutions. In *Asphaltene, Heavy Oils and Petroleomics*; Mullins, O. C., Sheu, E. Y., Hammami, A., Marshall, A. G., Eds.; Springer: New York, 2007; Chapter 18.

(44) Oh, K.; Deo, M. D. Near infrared spectroscopy to study asphaltene aggregation solvents. In *Asphaltene, Heavy Oils and Petroleomics*; Mullins, O. C., Sheu, E. Y., Hammami, A., Marshall, A. G., Eds.; Springer: New York, 2007; Chapter 19.

(45) Friberg, S. E.; Al Bawab, A.; Abdoh, A. A. Surface active inverse micelles. *Colloid Polym. Sci.* **2007**, *285*, 1625–1630.

(46) Mullins, O. C. Petroleomics and structure–function relations of crude oils and asphaltenes. In *Asphaltene, Heavy Oils and Petroleomics*; Mullins, O. C., Sheu, E. Y., Hammami, A., Marshall, A. G., Eds.; Springer: New York, 2007; Chapter 1.

(47) Fotland, P.; Anfinsen, H. Conductivity of asphaltenes. In *Structures and Dynamics of Asphaltenes*; Mullins, O. C., Sheu, E. Y., Eds.; Plenum Press: New York, 1998; Chapter 8.

(48) Barsoukov, E.; Macdonald, J. R. *Impedance Spectroscopy, Theory, Experiment and Application*, 2nd ed.; Wiley Interscience: New York, 2005; p 187.

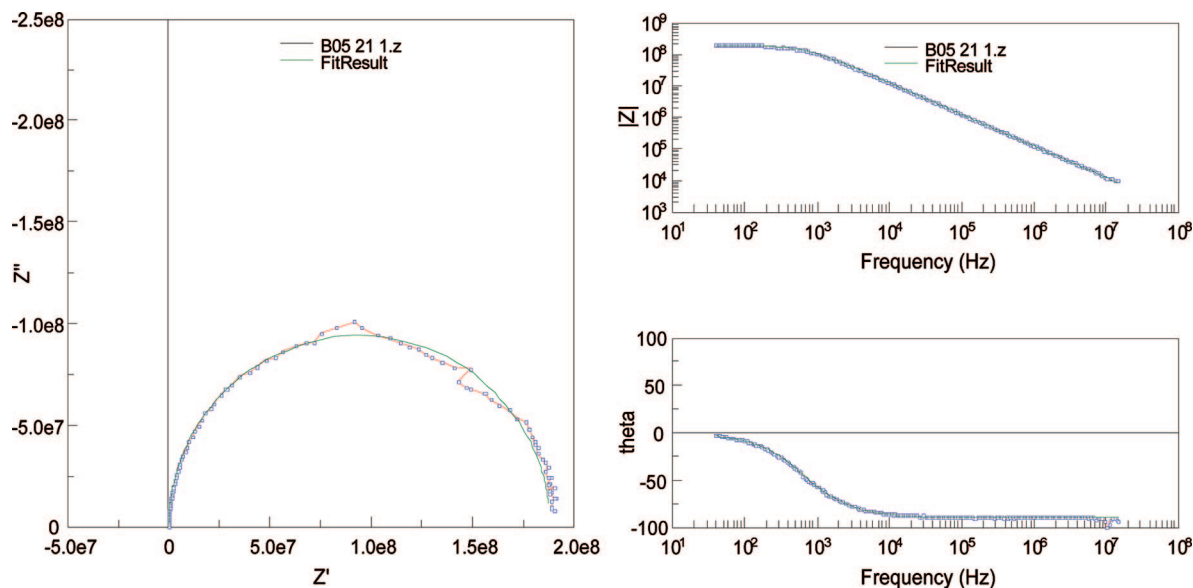


Figure 2. Nyquist plot (left) shows the relationship between the imaginary part (Z'') and the real part (Z') of the impedance, and the Bode plots (right) show the frequency dependences of the magnitude and phase angle of the complex impedance. The data (red) are for UG8 asphaltene in toluene at 0.5 g/L (21 °C). These plots establish the validity of the model circuit (Figure 1) and also establish the frequency limits for purely resistive impedance. The unit of z' , z'' , and $|z|$ is ohm. The unit of theta is degree.

Table 1. Measured Dielectric Constants of Several Organic Solvents and Water at 21 °C

	measured	literature ⁵⁵
toluene	2.41	2.38
<i>n</i> -heptane	1.96	1.92
<i>n</i> -pentane	1.83	1.84
pyridine	12.4	12.3
water	78.9	80.1

Table 2. Measured Electrical Conductivity of NaCl Solution at 21 °C ($\mu\text{S cm}^{-1}$)

	measured	literature ⁵⁶	literature ⁵⁷
0.5 mM NaCl—H ₂ O	56.98	55.55(21 °C)	62.22 (25 °C)

platinum-plate electrical conductivity cell (CS SK 21-T from Topac, Irvine, CA; cell constant: 0.1 s cm⁻¹) on an Agilent 4294A impedance analyzer at room temperature (21 °C). The sweeping frequency range was from 40 Hz to 15 MHz, and the oscillator level was set at 500 mV, while the direct current (DC) bias was set to zero.

Prior to the measurement, both open- and short-compensation were conducted on the impedance analyzer with the conductivity cell connected and the data were stored on the instrument for automatic compensation during the subsequent measurements. After the measurements, the measured data were imported into software for electrochemical impedance analysis, ZView (Scribner, Southern Pines, NC), to find estimates of all of the parameters using a suitable equivalent circuit.

For impedance measurements of liquid by the parallel plate method employed in this study, an equivalent circuit composed of a resistor (R_p) parallel to a capacitor (C_p) was used (Figure 1).⁴⁹ For such a parallel R – C circuit, the measured impedance (Z) and phase angle (θ) will change with frequency, f ⁵⁰

$$Z = \frac{R_p}{1 + j2\pi f R_p C_p} \quad (1)$$

$$\theta = \tan^{-1}(2\pi f R_p C_p) \quad (2)$$

(49) Agilent Technologies. Agilent solutions for measuring permittivity and permeability with LCR meters and impedance. Agilent Application Note 1369-1, 2007.

(50) Henry, R. W. *Electronic Systems and Instrumentation*; John Wiley and Sons, Inc.: New York, 1978, p 75.

When the frequency is much less than $1/2\pi R_p C_p$, the magnitude of the impedance will be approximately equal to R_p . For higher frequency, then, the impedance value will be a combination of both R_p and C_p .

For this parallel R – C circuit, if the imaginary part of impedance, Z'' , is plotted against the real part, Z' (Nyquist plot), a characteristic semicircle will be shown. Characteristic Bode plots can also be obtained when one plots the absolute values of impedance, $|Z|$, or phase angle against the frequency.⁵¹

A typical result for our measurement is shown in Figure 2. This is for a solution of UG8 asphaltene in toluene at 0.5 g/L. From the figure, one can clearly see that the Bode and Nyquist plots are as expected for a parallel R – C circuit. This validates the use of a parallel R – C circuit for the measurement on asphaltene toluene solutions.

To check the reliability of the measured data, dielectric constants, ϵ_r , of several organic solvents as well as water are obtained from measured equivalent parallel capacitance, C_p , as listed in Table 1, according to

$$\epsilon_r = \frac{l C_p}{A \epsilon_0} \quad (3)$$

in which l is the distance between the two electrodes, A is the surface area of the electrodes, and ϵ_0 is the permittivity of free space, which is 8.854×10^{-12} F/m. Table 1 shows that the measured values are very close to the literature values.

The estimated equivalent parallel resistance value (R_p) was then converted into a DC electrical conductivity value of the sample (σ) using

$$\sigma = \frac{l}{A R_p} \quad (4)$$

The electrical conductivity of NaCl solution of 0.5 mM was also measured (Table 2) and shown to be very close to literature values.

(51) Gamry Instruments. Basics of electrical impedance spectroscopy, 2007.

(52) Khvostichenko, D. S.; Andersen, S. I. Interactions between asphaltenes and water in solutions in toluene. *Energy Fuels* **2008**, 22, 3096–3103.

(53) Fawcett, W. R. Thermodynamic parameters for the salvation of monatomic ions in water. *J. Phys. Chem. B* **1999**, 103, 11181–11185.

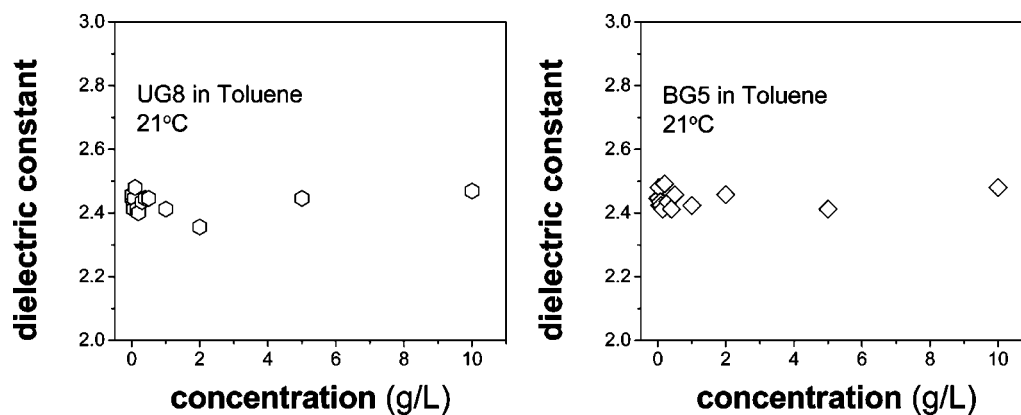


Figure 3. Dielectric constants of UG8–toluene (left, hexagon) and BG5–toluene (right, rhombus) solutions at 21 °C as a function of asphaltene concentration.

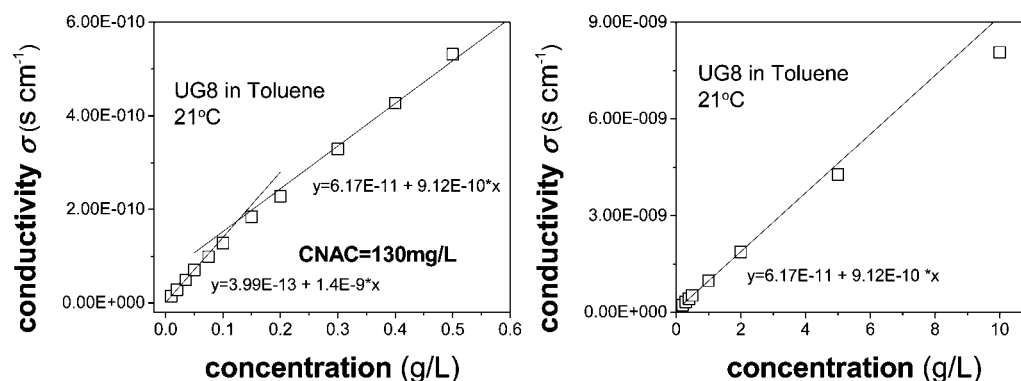


Figure 4. DC conductivity of UG8 asphaltene in toluene. The plot on the left shows the CNAC as the break in the curve at 130 mg/L. The plot on the right shows that there is no change in the slope of the conductivity curve above the CNAC up to 2 g/L. The higher concentrations show a deviation from this slope because of nanoaggregate clustering.

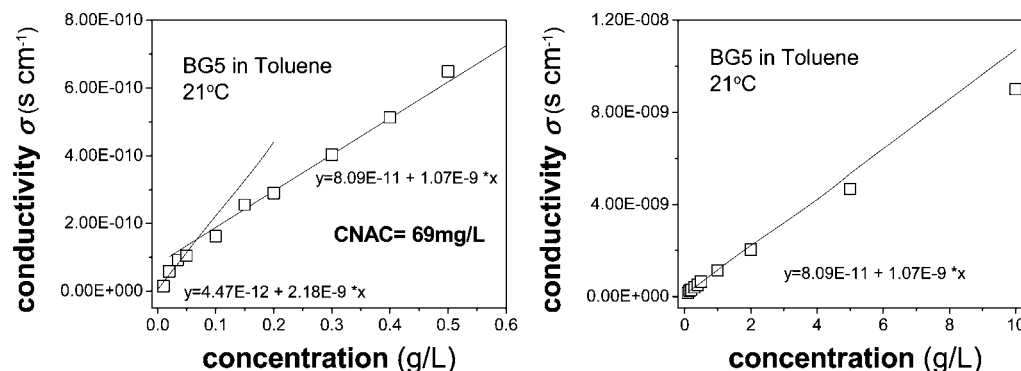


Figure 5. DC conductivity of BG5 asphaltene in toluene. The plot on the left shows the CNAC as the break in the curve at 69 mg/L. The plot on the right shows that there is no change in the slope of the conductivity curve above the CNAC up to 2 g/L. The higher concentrations show a deviation from this slope because of nanoaggregate clustering.

Thus, the electrical conductivity and capacity values obtained by this method are reliable.

Previous AC conductivity measurements measured impedance values at one⁴⁷ or several frequencies.³² In this study, we used the low-frequency electrical impedance technique plus a parallel R – C circuit model to fit the impedance values in a broad frequency range. The fitting results agree with the model well and give the characteristic DC electrical conductivity and dielectric constant values.

Results and Discussion

Figure 3 gives the dielectric constants of UG8 and BG5 asphaltene solutions in toluene. The values are all close to the

value of pure toluene. It shows that the existence of asphaltene at the concentrations under investigation did not change the dielectric constant of the solutions.

Figure 4 shows the low-frequency conductivity of UG8 asphaltene in toluene as a function of the concentration. The points at 100 mg/L and lower fall on a straight line. Above 150 mg/L, up to 2 g/L, the conductivity points fall on a line of smaller slope. We interpret these data to represent a change in asphaltene aggregation at ~ 130 mg/L for this asphaltene. Figure 5 shows equivalent data for BG5 asphaltene; again, there is a straight line section at low concentration and a second straight line concentration range at higher concentrations. The change in slope for BG5 asphaltene occurs at ~ 69 mg/L. This asphaltene appears to aggregate at a somewhat lower concentration. For both UG8 asphaltene (Figure 4) and BG5 asphaltene (Figure 5), the conductivity–concentration curves show a

(54) Izutsu, K. *Electrochemistry in Nonaqueous Solutions*; Wiley-VCH: New York, 2002; pp 5–8.

(55) *CRC Handbook of Chemistry and Physics*, 88th ed.; Lide, D. R., Ed.; CRC Press: Boca Raton, FL, 2007; pp 6–148.

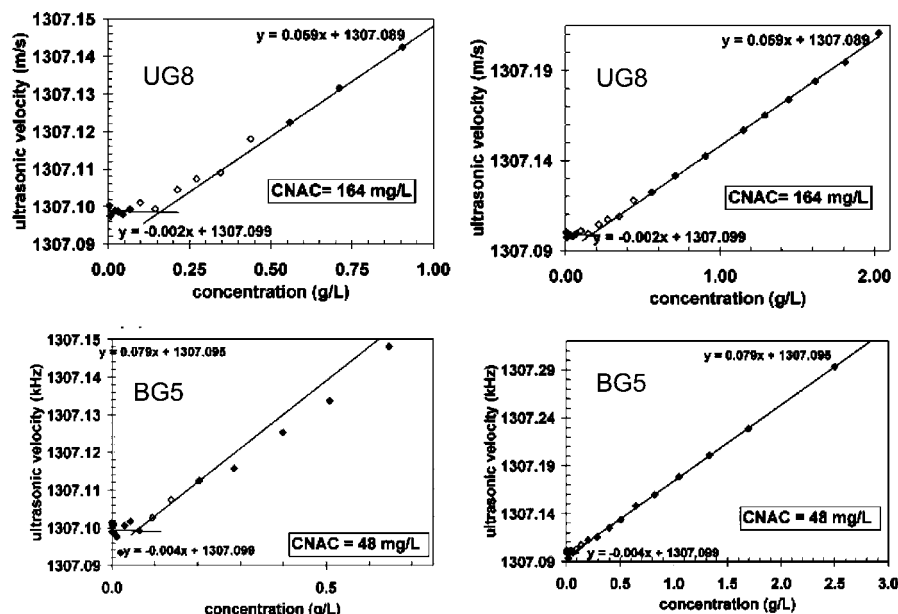


Figure 6. High- Q ultrasonic data show the CNAC for UG8 asphaltene at 164 mg/L and for BG5 asphaltene at 48 mg/L. This figure was obtained with permission from ref 31. Remarkably, this is a close match to the conductivity data in Figures 4 and 5.

“bend” above 5 g/L, which might be due to the clustering of asphaltene at higher concentrations. This is consistent with the findings of nanoaggregate clustering at this concentration.^{43,44} A further investigation will be conducted for this phenomenon.

Figure 6 shows data from the early high- Q ultrasonic studies.^{30,31} The ultrasonic velocity versus the asphaltene concentration is determined by the compressibility of asphaltene monomers in solution below CNAC and the compressibility of nanoaggregates above CNAC. The break in the ultrasonic velocity curves gives the CNAC. In a remarkable finding, the CNACs determined from the ultrasonic curves in Figure 6, 164 mg/L for UG8 asphaltene and 48 mg/L BG5 asphaltene, closely match the corresponding CNACs from the conductivity data shown in Figures 4 and 5. Some of the reported differences in the CNACs from different techniques are evidently due to the different asphaltenes used, having been obtained from different oil samples. In addition, both the low-frequency conductivity curves and the ultrasonic velocity curves show no further change in slope above CNAC up to concentrations of several grams per liter. The implication is that the nanoaggregates do not change size up to this concentration, but rather, the addition of more asphaltene simply causes an increased number of nanoaggregates. The reported cluster formation of asphaltenes at concentrations of several grams per liter^{43,44} is not fully understood and will be the subject of future studies. Nevertheless, we note that our data show a reduction of slope at a concentration of several grams per liter; therefore, our data are consistent with previous reports that asphaltene nanoaggregates form clusters at several grams per liter.^{43,44}

As noted in the Experimental Section, the charge carriers responsible for the conduction in these experiments are monopole charges as opposed to dipole charges. That is, the 40 Hz frequency used in these experiments is on the frequency-independent plateau of the Bode plot and, thus, cannot be capacitive. In addition, the phase angle is virtually zero at this frequency. Figure 7 shows the relative conductiv-

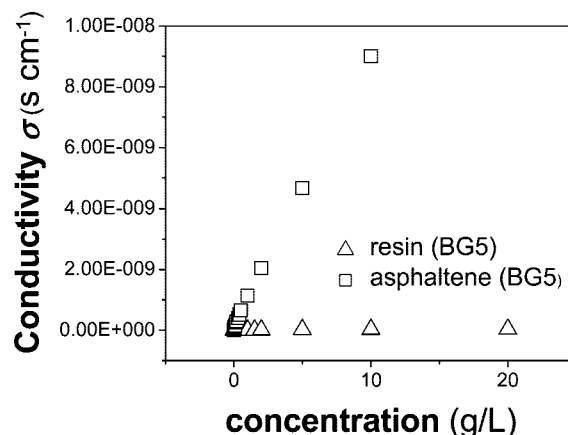


Figure 7. Electric conductivities of BG5 asphaltene (\square) and BG5 resin (Δ) in toluene at 21 °C.

ity of resins versus asphaltenes for BG5 asphaltene. As expected, the asphaltenes have a much higher concentration of charge carriers (in toluene) than the resins. This is consistent with the higher heteroatom content of asphaltenes as well as their higher interfacial activity. We note that crude oils when washed with water yield water-soluble components that are ionized as shown by ultra-high-resolution mass spectroscopy.³ These species are not dissimilar to the petrogenic, biodegraded, asphaltene-derived components found ubiquitously in the hydrosphere of the earth.² We assume that the ionized asphaltene molecules in toluene are large organic ions with some charge stabilization mechanism at play. For example, basic, aromatic nitrogen is a large mass fraction of asphaltene nitrogen.⁴¹ Protonation of this nitrogen allows for some delocalization of the charge. The organic acids most commonly found are carboxylic acids, possibly associated with some waters of hydration in toluene. Dispersed water in toluene has been noted to impact asphaltene aggregation.⁵² Sulfonic acids, while very low in concentration in asphaltenes, might be found in the water-soluble components of crude oils.³

The order-of-magnitude concentration of these charge carriers in asphaltenes can easily be determined. Validation of this determination is obtained by a comparison to measurements of

(56) Chinese National Standard for Machinery Industry. Test solutions of electric conductivity analyzers. Preparation method of sodium chloride solutions. JB/T 8278-1999, 1999.

(57) *CRC Handbook of Chemistry and Physics*, 88th ed.; Lide, D. R., Ed.; CRC Press: Boca Raton, FL, 2007; pp 5–75.

known salt solutions in water. For the aqueous solution of sodium chloride, because

$$\sigma_{\text{NaCl}} = \sigma_{\text{Na}^+} + \sigma_{\text{Cl}^-} \quad (5)$$

and the electric conductivities of Na^+ and Cl^- are related to their sizes

$$\frac{\sigma_{\text{Na}^+}}{\sigma_{\text{Cl}^-}} = \frac{r_{\text{Cl}^-}}{r_{\text{Na}^+}} \quad (6)$$

The crystal radii of Na^+ , r_{Na^+} , obtained from X-ray crystallographic data, is 116 pm, and the crystal radii of Cl^- , r_{Cl^-} , is 167 pm,⁵³ therefore

$$\sigma_{\text{Cl}^-} = 0.59\sigma_{\text{NaCl}} \quad (7)$$

If we assume one asphaltene molecule has one negative charge, the viscosity of toluene is 0.553 cP, and the viscosity of water is 0.890 cP,⁵⁴ then

$$\frac{\sigma_{\text{Cl}^-}}{\sigma_{\text{asp}}} = \frac{\eta_{\text{toluene}}}{\eta_{\text{water}}} \frac{n_{\text{Cl}^-}}{n_{\text{asp}}} \frac{r_{\text{asp}}}{r_{\text{Cl}^-}} = 0.62 \frac{n_{\text{Cl}^-}}{n_{\text{asp}}} \frac{r_{\text{asp}}}{r_{\text{Cl}^-}} \quad (8)$$

in which η is the viscosity, n_{Cl^-} is the number of Cl^- ions in the solution, and n_{asp} is the number of charged asphaltene particles in the solution.

For NaCl of 0.1 mM, $\sigma_{\text{NaCl}} = 2.07 \times 10^{-5} \text{ S cm}^{-1}$; therefore, $\sigma_{\text{Cl}^-} = 1.22 \times 10^{-5} \text{ S cm}^{-1}$. For asphaltene of 0.1 mM (use 750 g/mol as the average molecular weight for asphaltene), $\sigma_{\text{asp}} = 9.9 \times 10^{-11} \text{ S cm}^{-1}$. If we take the radius of an asphaltene monomer as $r_{\text{asp}} = 1 \text{ nm}$, then

$$\frac{n_{\text{Cl}^-}}{n_{\text{asp}}} = 3.2 \times 10^4 \quad (9)$$

because

$$n_{\text{Cl}^-} = C_{\text{NaCl}} \text{vol} K_A \quad (10)$$

$$n_{\text{asp}} = C_{\text{total asp}} C_{\text{charge}} \text{vol} K_A \quad (11)$$

in which $C_{\text{total asp}}$ is the concentration of total asphaltene, C_{charge} is the concentration of charge carriers in total asphaltene particles, vol, is the volume of testing liquid between two electrodes, and K_A is the Avogadro constant. If $C_{\text{NaCl}} = C_{\text{total asp}} = 0.1 \text{ mM}$, then we can obtain

$$C_{\text{charge}} = 3.1 \times 10^{-5}$$

Using the known average molecular weight of these asphaltene specifically (and all virgin crude oil asphaltene in general), we obtain a fraction of ionized asphaltene molecules as $\sim 10^{-5}$. Crude oils can consist of percent levels of acids;³ however, it is much less likely that these ionize in toluene.

Note that this estimate is sensitive to our assumption that $r_{\text{asp}} = 1 \text{ nm}$ and that r_{Cl^-} is approximately equal to the crystal radii value. However, even if the monomer size is an order of magnitude larger than this, we would have $C_{\text{charge}} \sim 10^{-4}$, still a very small fraction indeed.

We assume that the charge carriers in asphaltene solutions in toluene are (separated) large organic ions. Upon nanoaggregate formation, we assume that a given ionic molecule associates with neutral molecules only. With this model, we can use the change in slope at the CNAC to give the aggregation number. Equation 12 describes the force balance for ionic conduction

$$qE = 6\pi\eta rv \quad (12)$$

where q is the charge, E is the electric field, η is viscosity, r is the ion radius, and v is the velocity of the charged particle. The velocity of the molecule versus nanoaggregate is different by virtue of their radius. At the CNAC, only the radius r changes. This model of conductivity is distinct from the standard micelle theory, where monodispersity is presumed. The cube of the ratio of the radii before and after CNAC gives an estimate of the aggregation number. For UG8, we obtain 3.5, and for BG5, we obtain 8.4. The primary point is that the aggregation number is small. This conclusion has been reached by NMR diffusion studies⁹ and analysis of the asphaltene gradients in oilfield oil columns using equations of state modeling.³⁵ Such small aggregation numbers that are in sharp contrast to the large aggregation number of most aqueous micelles have been argued to derive from fundamental asphaltene molecular properties.³⁰ For example, the aggregation number of sodium dodecyl sulfate in water is 60.⁵⁸ We note that the molecularly dispersed ions might be associated with waters of hydration or potentially with a dipole of another molecule below CNAC, so that the change in slope provides only an approximate aggregation number. In any event, the congruence of the conductivity data of Figures 4 and 5 and the ultrasonic data of Figure 6 indicate that the ionic species behave similarly to the neutrals regarding aggregation. In addition, in a general sense, the results from these conductivity experiments yield similar results to all recent studies of asphaltene nanoaggregates, including high- Q ultrasonics, AC conductivity (where asphaltene dipole moments created the measured effects), NMR, centrifugation, and field studies of asphaltene gradients. Evidently, the small ionic molecular fraction of asphaltene can be used as a tracer to understand aggregation properties of asphaltene.

Conclusions

Asphaltene nanoaggregate formation is now firmly established as one of their defining properties. In addition, there is a limited but real difference in CNACs of different asphaltene. Different techniques can now be used to explore subtleties of this aggregation process. In general, the definition of a toluene-soluble and *n*-heptane-insoluble asphaltene is not arbitrary but carries chemical meaning. Toluene solubility captures the most aromatic components of crude oils, and *n*-heptane insolubility largely captures the fraction of crude oil that forms nanoaggregates. In the general effort to delineate asphaltene properties, widely different source materials, such as coal, have been used. It is now necessary to determine the aggregation properties of these different asphaltene. The objective is to find invariants for the asphaltene solubility class especially when chemical identity varies. In this way, asphaltene identity will at last be revealed.

Acknowledgment. We thank Dr. Nikita Seleznev (Schlumberger-Doll Research) and Dr. Deyang Qu (University of Massachusetts—Boston) for their kind help.

EF800781A

(58) Turro, N. J.; Yekta, A. Luminescent probes for detergent solutions. A simple procedure for determination of the mean aggregation number of micelles. *J. Am. Chem. Soc.* **1978**, *100*, 5951.